NEUTRON CAPTURE BY NEODYMIUM ISOTOPES

THE CAPTURE CROSS-SECTIONS OF NEODYMIUM ISOTOPES FOR PILE NEUTRONS

By

WILLIAM HERBERT WALKER, B.A. Sc.

A Thesis

Submitted to the Faculty of Arts and Science

in Partial Fulfilment of the Requirements

for the Degree

Master of Science

McMaster University

October, 1952

MASTER OF SCIENCE (1952)
(Physics)

McMASTER UNIVERSITY
Hamilton, Ontario

TITLE: The Capture Cross-sections of Neodymium Isotopes for Pile Neutrons

AUTHOR: William Herbert Walker, B.A.Sc. (Toronto)

SUPERVISOR: Professor H. G. Thode

NUMBER OF PAGES: 48

SCOPE AND CONTENTS:

A Dempster-type double-focussing mass spectrometer has been used to determine the relative abundances of the isotopes of neodymium using two samples, one irradiated in a strong neutron flux, the other, obtained from the same source, unirradiated. A comparison of these results permits the calculation of the cross-section of each isotope for the capture of pile neutrons. Results previously obtained have been extended to give definite cross-sections for three of the isotopes, two of which have not previously been reported, and to lower the upper limits for the remainder.

ACKNOWLEDGEMENTS

The author wishes to acknowledge the encouragement of Professor H. G. Thode, under whose direction this work has been done.

He is indebted, also, to Dr. R. H. Tomlinson for his guidance in developing suitable purification techniques in the preparation of neodymium oxalate, and to Dr. D. M. Shaw, who analyzed the neodymium for the presence of praseodymium, using the twenty-one foot grating spectrograph.

The generous financial assistance of the Atomic Energy of Canada Limited has made this work possible.

CAPTURE CROSS-SECTIONS OF NEODYMIUM ISOTOPES

FOR PILE NEUTRONS

TABLE OF CONTENTS

Section	Subject	Page
(I)	Introduction	1
(II)	Theory of Isotope Redistribution During Irradiation	4
(III)	Apparatus	8
	(1) Principle of Operation	8
	(2) Source	10
	(3) Deflectors	10
	(4) Collector	13
	(5) Vacuum System	13
	(6) Electronics	14
(IV)	Experimentation	15
	(1) Sample Preparation	15
	(2) Operating Conditions	16
	(3) Resolution and Peak Shape	17
(V)	Results	19
	(1) Treatment of Results	19
	(a) Measurement of peak height.....	19
	(b) Calculation of relative abundance..	19
	(2) Unirradiated Nd-Metal Filings Sample....	21
	(3) Unirradiated Nd - Oxalate Sample	23
	(4) Irradiated Nd - Oxalate Sample	24

CAPTURE CROSS-SECTIONS OF NEODYMIUM ISOTOPES

FOR PILE NEUTRONS

TABLE OF CONTENTS

Section	Subject	Page
(V) cont.	(5) Capture Cross-sections for Pile Neutrons	25
	(a) First Order Approximation	25
	(b) Exact Equations	26
	(6) Corrections for Gains & Losses.....	27
	(7) Corrections for Contamination	29
(VI)	Discussion	32
Appendices	A - Derivation of Cross-Section Equations..	35
	B - Resolution & Peak Shape	41
Tables ..	I - Results for Unirradiated Nd (Filings)	22
	II -Results for Unirradiated Nd (Oxalate)	23
	III-Results for Irradiated Nd (Oxalate)	25
	IV -Isotopic Capture Cross-Sections	26
	V -Isotopic Abundances for Naturally-occurring Nd	32
	VI -Comparison of Results for Isotopic Cross-Sections	34

LIST OF ILLUSTRATIONS

FIG.	SUBJECT	PAGE
Fig. 1	- Double-focussing Mass Spectrometer	9
2	- Crucible-type Spectrometer Source	11
3	- Adjustable Slit and Collector	12
4	- Sample Set of Neodymium Peaks	20
A1	- Dimensions of Double-Focussing Spectrometer	42
A2	- Resolution of Mass Mo Peaks	43
A3	- Peak Shape: Variation with Relative Slit Width	46

I. INTRODUCTION

The absorption, or capture, of a neutron by a nucleus is not usually followed by particle emission*. The product nucleus is, therefore, an isotope of the product element having one additional neutron. The binding energy of the neutron + is released in the form of gamma-rays; hence the name "radiative capture".

The radiative absorption cross-sections of individual isotopes may be measured in several ways.

(i) Activation: If an element having several isotopes is irradiated with neutrons the product will contain both stable and radioactive nuclei. One of the most fruitful methods used to date has been the determination of cross-sections leading to radioactive nuclei, commonly referred to as "activation cross-sections". In this method the intensity of the radioactivity of the product is measured. If the counter geometry, incident neutron flux, half-lives and modes of decay of the products are known, then the capture cross-section can be calculated. The most comprehensive work in this field has been done by Seren, Friedlander, and Turkel[1]. They estimate the maximum obtainable accuracy to be 10%. The minimum measurable cross-section depends not only on its magnitude, but also on the intensity, energy, and mode of the subsequent radioactive decay. The smallest cross-section reported is 0.0002 barns (1 barn = 10^{-24} cm^2).

---

* There are several exceptions at low masses, e.g. $Li^6(n,\alpha)H^3$, $B^{10}(n,\alpha)Li^7$, $N^{14}(n,p)C^{14}$.

+ The binding energy of a neutron in a nucleus is equal to the difference between the mass of the target nucleus plus mass of the free neutron, and the mass of the product nucleus.

(ii) Pile Oscillator: A second method of more recent development will increase in importance as isotopically-enriched elements become more readily available. A neutron absorber, the element under study, is moved back and forth in a field of thermal neutrons. In the vicinity of the absorber there will be a depression in the neutron flux, the movement of which depression is recorded as it passes an ionization chamber. The oscillating signal has an amplitude proportional to the absorption cross-section of the sample. By comparing several samples of one element, each having a different isotopic enrichment, the absorption cross-sections of all the isotopes can be determined. Several elements have been surveyed by this method, particularly certain metals[2,3,4]. The minimum cross-section measured has been about 0.1 barns, with an accuracy of 25%. This improves to 5% for values greater than 5 barns.

(iii) Absorption: The use of velocity selectors[5], or crystal monochromators[6], in which the attenuation of a beam of neutrons of known energy is measured, will also yield isotopic capture cross-sections when used with monoisotopic or isotopically-enriched elements. In this case the variation of cross-section with energy can be determined, where all other methods described here give a cross-section over a distribution of neutron energies.

(iv) Mass Spectrometer: Considerable work has also been done by measuring the changes in the isotopic abundances due to neutron capture, using a mass spectrometer[7,8,9,10]. This is the method employed in the present experiment. Limiting cross-section measurement and accuracy are determined by the total irradiation (flux x time) and the sensitivity of the

mass spectrometric technique.

A number of elements were irradiated near the centre of the NRX pile at Chalk River. Of these, neodymium was chosen as most suitable for evolving satisfactory techniques because of its high thermal ionization efficiency*.

The isotopic cross-sections of neodymium have been studied previously, both by activation methods[11] and with a mass spectrometer[10]. Since greater accuracy was expected in the present experiment due to the very high neutron flux available in the NRX pile, it was felt that these previous results could be considerably extended and improved. Such was the case. In addition to the large cross-section assigned to Nd^{143} by Hess and Ingraham, two other lesser cross-sections were established (Nd^{142} and Nd^{145}), and the upper limits for all other isotopes were considerably reduced.

---

*Ionization efficiency of an ion source is defined as the ratio of the no. of atoms emitted in a charged state to those emitted in a neutral state.

II. THEORY OF ISOTOPE REDISTRIBUTION DURING IRRADIATION

The rate at which neutrons are absorbed by the target nuclei is measured in terms of the "capture cross-section". If a beam of N neutrons per sec., 1 cm. square, passes thru a target containing M nuclei per cm^2 of surface area perpendicular to the incident beam, where σ is the capture cross-section per nucleus,

then the number of capture events per sec. = N. M. σ

whence $$\sigma = \frac{\text{number of capture events per nucleus}}{\text{number of incident neutrons}}$$

In classical terms, the probability of capture per nucleus per sec. is equal to the ratio of the "area" of the nucleon to 1 $cm.^2$ (both perpendicular to the neutron beam) times the number of incident neutrons per sec. per $cm.^2$ The conventional unit for σ is the "barn". (1 barn = $10^{-24} cm^2$).

In order to determine the mass redistribution, following irradiation, for an element with isotopes of mass A_1, A_2, ----, A_n, having cross-sections σ_1, σ_2, ---, σ_n, it is necessary to treat each isotope as the parent of a "capture chain", in analogy to the "radioactive chain" of the massive elements, or of fission products. The number of nuclei of the s^{th} isotope, after an irradiation for time, t, will be

n'_s = original number of S^{th} nuclei (n_s) less the number which captured neutrons

+ the number of S^{th} neutrons arising from capture by the $(S-1)^{th}$ nuclei
+ the number of S^{th} neutrons arising from capture by the $(S-2)^{th}$ nuclei followed by capture (a small proportion) by the $(S-1)^{th}$ nuclei.

The general formula for the number of nuclei of the S^{th} product of a radioactive series is -

$$(1)\qquad n_s' = n_1 \lambda_1 \lambda_2 \cdots \lambda_{s-1} \left[\frac{e^{-\lambda_1 t}}{(\lambda_2-\lambda_1)(\lambda_3-\lambda_1)\cdots(\lambda_s-\lambda_1)} + \frac{e^{-\lambda_2 t}}{(\lambda_1-\lambda_2)(\lambda_3-\lambda_2)\cdots(\lambda_s-\lambda_2)} + \cdots + \frac{e^{-\lambda_s t}}{(\lambda_1-\lambda_s)(\lambda_2-\lambda_s)\cdots(\lambda_{s-1}-\lambda_s)} \right]$$

To convert to neutron capture, it is necessary to replace the decay constants. Since λ = the probability of a nucleus decaying per sec., the replacement will be σN, the probability of a nucleus capturing per sec.

As an example, the equation for the capture cross-section of the third isotope will be derived. Applying equation (1) to the 3rd, 2nd, and 1st isotopes succesively, the number of nuclei after irradiation is

$$(2)\qquad n_3' = n_3 e^{-\sigma_3 N t} + n_2 \sigma_2 \left[\frac{e^{-\sigma_2 N t}}{\sigma_3-\sigma_2} + \frac{e^{-\sigma_3 N t}}{\sigma_2-\sigma_3} \right] + n_1 \sigma_1 \sigma_2 \left[\frac{e^{-\sigma_1 N t}}{(\sigma_2-\sigma_1)(\sigma_3-\sigma_1)} + \frac{e^{-\sigma_2 N t}}{(\sigma_1-\sigma_2)(\sigma_3-\sigma_2)} + \frac{e^{-\sigma_3 N t}}{(\sigma_1-\sigma_3)(\sigma_2-\sigma_3)} \right]$$

where n_1, n_2 and n_3 are the initial numbers of nuclei of the 1st, 2nd and 3rd isotopes respectively. In Appendix A the detailed development of this and the associated equations is treated. It is shown there how equation (2) may be rearranged to give the equation for σ_3.

$$(3)\qquad \sigma_3 N t = ln\left[n_3 + \frac{n_2 \sigma_2}{(\sigma_2-\sigma_3)} + \frac{n_1 \sigma_1 \sigma_2}{(\sigma_1-\sigma_3)(\sigma_2-\sigma_3)} \right] - ln\left[n_3' + \frac{n_2' \sigma_2}{(\sigma_2-\sigma_3)} + \frac{n_1' \sigma_1 \sigma_2}{(\sigma_1-\sigma_3)(\sigma_2-\sigma_3)} \right]$$

A considerable simplification can be effected if the net change in the abundance of an isotope is small. If it is assumed that the rate of change is constant with time, rather than exponential, the cross-section equations become (as shown in Appendix A)

$$(4)\qquad \begin{aligned} \sigma_1 N t &= \Delta n_1 \,/\, \tfrac{1}{2}(n_1 + n_1') \\ \sigma_2 N t &= \Delta n_2 \,/\, \tfrac{1}{2}(n_2 + n_2') \end{aligned}$$

where $\Delta n = n - n'$. etc.

The above equations have been developed in terms of numbers of nuclei. As long as the total number of nuclei within the element remains unchanged, no correction is required if the percent relative abundance of each isotope is used instead of the number of nuclei. Nuclei will be lost to the element whenever an unstable isotope is formed in capture, since some or all of these nuclei will decay to another element. Nuclei will be gained if there is some contaminant which, after neutron capture and radioactive decay, yields an isotope of the element under study.

As a simple example of the result of loss of nuclei, consider the hypothetical case of two adjacent isotopes of equal initial abundance, and equal cross-sections. Let the initial number of nuclei be N each. Initial relative abundances will be 0.5 each. If x is the proportion each loses due to irradiation, the amount left will be N(1-x) and N nuclei. In addition there will be y nuclei of a third isotope, where y is less than Nx by an amount dependent on the radioactive half-life of the product. For convenience, let y = 0, indicating a half-life small compared to the time elapsed between irradiation and measurement. The final relative abundances will then be $(1-x) / (2-x) < 0.5$ and $1 / (2-x) > 0.5$, respectively.

Now the actual number of nuclei of the second isotope is unchanged. The formulae would show correctly, therefore, that its capture cross-section equalled that of the preceding isotope. But if relative abundances are used instead, the fact that the final abundance exceeds the initial indicates a smaller capture cross-section for the 2nd isotope.

Thus the uncorrected use of relative abundances can lead to erroneous values for the capture cross-sections. It will be necessary to examine the mass spectrometric data to determine whether either of these effects will make a significant change in the results.

III APPARATUS

The machine used here is a Dempster-type[12] double-focussing mass spectrometer, using a Shaw-type[13] crucible source for use with solids. It has been described in detail by R. J. Horsley[14]. The description of the instrument will, therefore, be brief, except where changes have been made.

1. Principle of Operation

As originally designed the spectrometer was dimensionally identical with Dempster's original mass spectrograph[12,15]. At about that time, the general theory of combinations of magnetic and radial electric fields was developed by Herzog[16], with particular emphasis on the optical analogy. Mattauch[17] used this work as a basis for discussing the special cases of radial electric field followed by a magnetic field which give "double-focussing". Where a simple magnetic spectrometer will focus a divergent monoenergetic beam, these special combinations, of which the Dempster machine is a particular example, will also give focussing where the beam is not monoenergetic. The former is called "direction-focussing", the latter "velocity-focussing". The optical analogue is the achromatic lens.

The independence of ion velocity is achieved in the following manner: If all ions have a fixed energy they will be focussed at one spot (A in Fig. 1) independent of mass. They will then diverge into the magnetic field and be refocussed, after passing through 180°, at B. Ions of a slightly greater mass will focus at C.

If the ions of a specific $\frac{e}{m}$ group are then given a slightly greater initial energy, they will focus at A′, to the left of A. In addition the radius of their orbit in the magnetic field will be greater.

After 180° they will focus at B′. By choosing the proper ratio for the radii of the central ion paths (a_e and a_m) it is possible to bring B′ into coincidence with B, as shown, thus achieving velocity focussing.

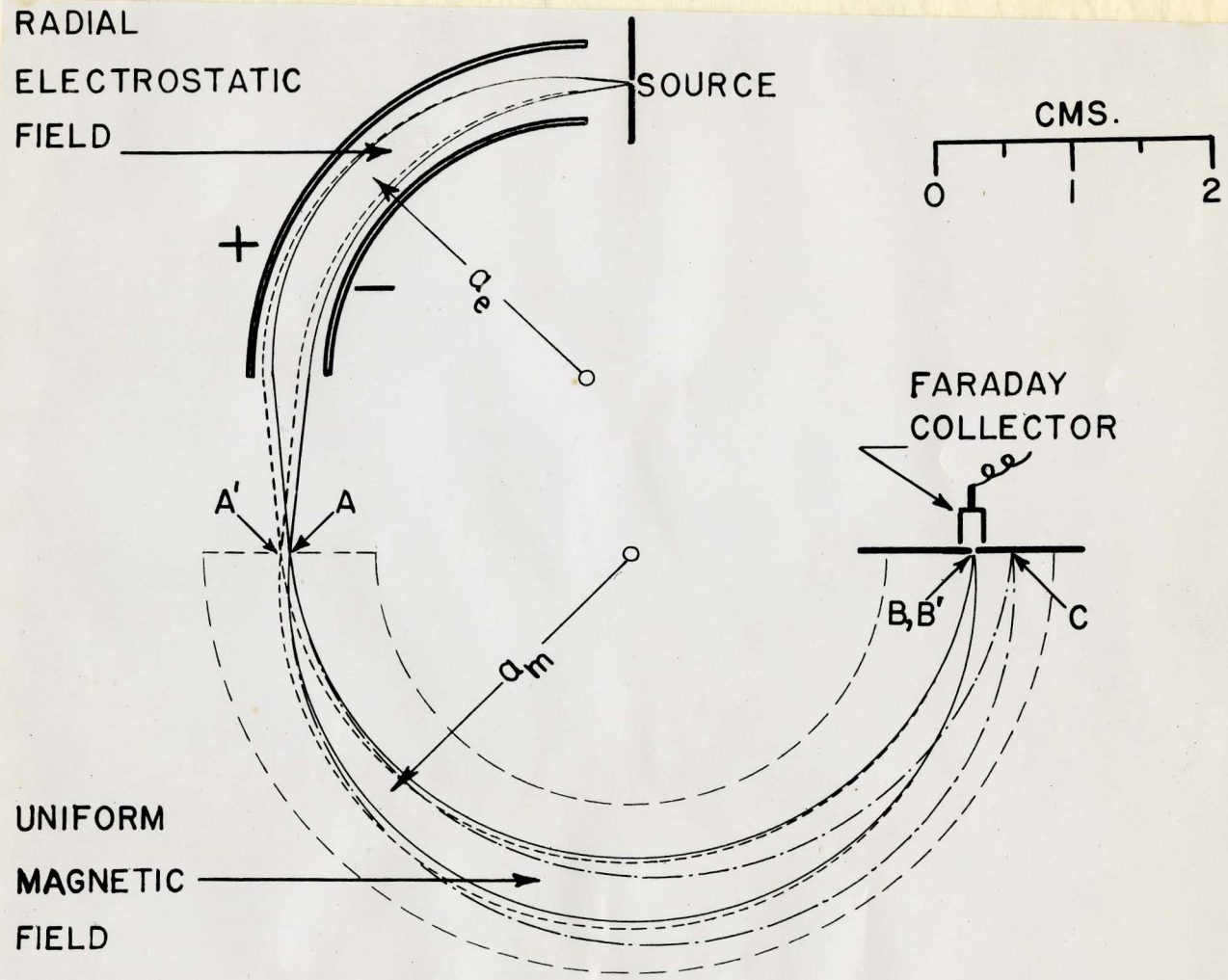

FIG. 1- DOUBLE-FOCUSSING MASS SPECTROMETER

The survey of a mass range is accomplished by steadily varying the magnetic field. Thus the heavier ions which are shown in focus at C would move towards B as the magnetic field increased. A Faraday cup at B connected to a D.C. amplifier, will then give a signal for the ions at B followed some time later by one for those ions initially at C.

2. Source

It was found that the "memory" of the spectrometer for past samples was traceable to the components of the source inside the shield. Such a memory persisted despite drastic chemical and mechanical cleaning. While the filament and crucible can be changed easily, and thus removed from the list of contaminators, the shield itself involved considerable machining, and therefore had to be treated as a semi-permanent part of the apparatus. Satisfactory results were obtained by protecting the inside of the shield with a metal liner (Fig. 2) consisting of a cylinder of Inconel tubing, a circular base of nichrome V, with central hole and cutaway for the crucible and filament supports respectively, and a circular nichrome V cap with central hole, through which passes the ion beam. Such an arrangement has no serious contaminations inherently, for neither nickel nor chromium have been identified with certainty. This is particularly true in the region of mass 150.

3. Deflectors

The electrostatic condenser plates, and the magnet pole faces have been fully described by Horsley[14]. The condenser plates have required occasional realigning because of jarring when taking the instrument apart.

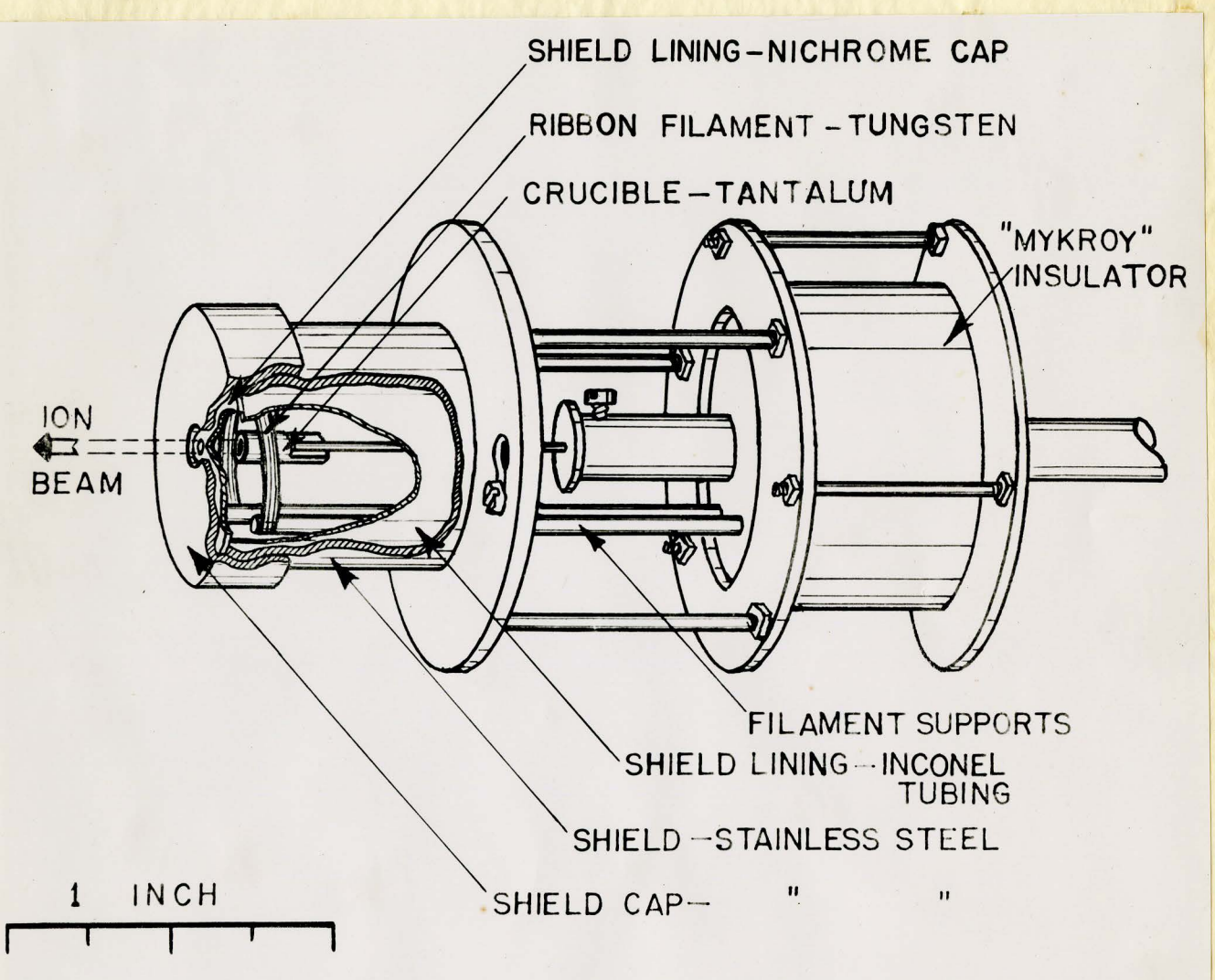

FIG. 2 – CRUCIBLE-TYPE SPECTROMETER SOURCE

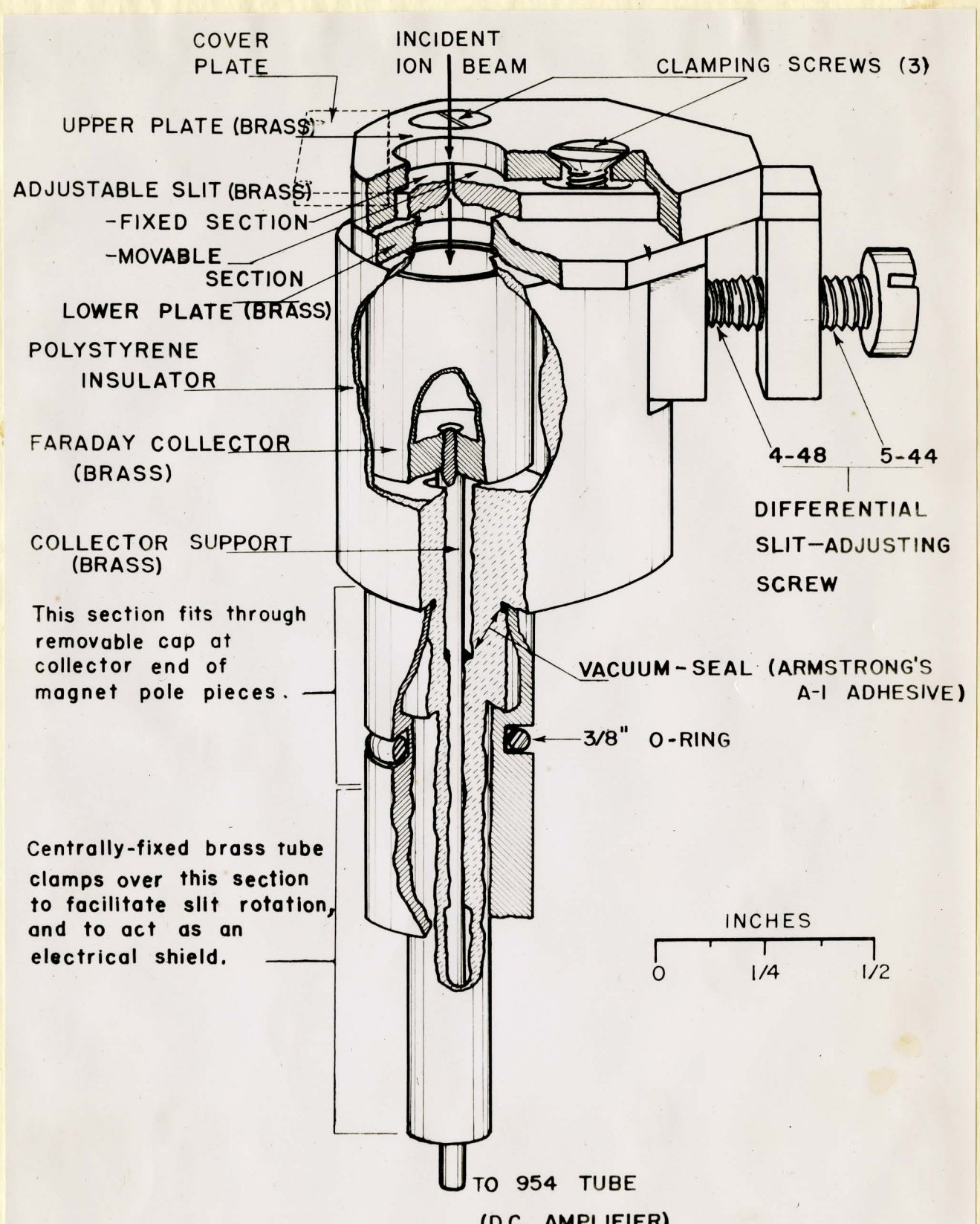

FIG. 3- ADJUSTABLE SLIT AND COLLECTOR

4. Collector

The collector was originally built with a fixed slit 0.3 mm. wide. Greater flexibility was required in the adjustment of resolution and peak width. Figure 3 shows the collector unit built to replace the original. It is situated so that the Faraday cup has the same position as before. The slit can be adjusted to any value by turning the differential screw, which was designed to give a slit width change of 0.05 mm per revolution. The whole unit can be rotated about the axis of the collector cup. By doing this while observing a peak, it is possible to determine the position for which the slit and beam are parallel, which orientation will give a peak of maximum height. The small plate which covers the edge of the collector holder was found necessary to eliminate both positive and negative secondary peaks caused by scattered ions and electrons produced when the beam passed along the inner surface of the polystyrene.

5. Vacuum System

A number of changes have been made in order to increase the pumping speed and minimize leakage at the joints. The mercury diffusion pump was replaced with an Edwards 03B two-stage oil-diffusion pump, rated at 50 litres per sec. In addition, the stopcock between diffusion pump and spectrometer was eliminated, and the glass tubing connecting the spectrometer to the pump was enlarged in diameter and shortened.

To improve joins between all metal sections of the spectrometer - between the electrostatic deflector and the magnet pole pieces, and between the latter and the removable collector assembly - the flat rubber gaskets used originally were replaced with O-rings. To do this it was necessary

to build up one or other of the metal surfaces with a brass ring, vacuum-sealed in place with Armstrong's A-1 Adhesive.

The glyptal seal of the magnetic deflector was replaced by black wax, Apiezon "W". It was found that a satisfactory seal could be obtained in the following manner: After thorough cleaning of all surfaces, the parts of the deflector were assembled. The unit was then placed in an oven and heated to about 180°F. After removal black wax was applied to all joins and screw holes with the use of an oxygen-gas flame.

6. Electronics

As described by Horsley[14], the unit supplying the bombarding electron current and accelerating voltage was limited to electron currents of 25 ma. or less. For the work with neodymium oxalate higher currents were necessary. This limitation was overcome by reducing the grid resistor of the control tube from 3,000 ohms to 200 ohms, permitting the removal of the "booster" transformer previously used. With this modification, a 2.5 cm. tungsten filament (cross-section 0.03" x 0.001") will provide bombarding electron currents greater than 50 ma. There is reason to doubt the reliability of the stabilizer at such currents and it may be advisable to replace the special transformer supplying the filament current.

IV EXPERIMENTATION

1. Sample Preparation

Two different sample preparations were used during the course of these experiments: neodymium metal filings, and neodymium oxalate. Despite marked isotope fractionation the metal filings yielded very satisfactory results (see table I). The use of the oxalate became necessary when the irradiated filings were found to be highly oxidized, and were not sufficient in quantity to permit repeated use in milligram amounts, as required with neodymium metal. Satisfactory techniques for using the oxalate in 50 to 100 microgram quantities were first evolved using unirradiated neodymium (see table II). All irradiated neodymium results were then obtained with the oxalate.

Simple preparation of the oxalate proved unsatisfactory because of the presence of contaminants, particularly iron. In order to obtain suitable ion emission from small samples it was necessary to purify the neodymium. About 5 mg. of neodymium were dissolved in a ml. of concentrated HCl. After evaporating to dryness, the residue was redissolved in a ml. of warm water. Neodymium oxalate was then precipitated by the addition of a ml. of oxalic acid, followed by gentle heating. The precipitate was next filtered out, and washed several times with warm water. Finally, the oxalate was redissolved by repeated washing with a small amount of concentrated HCl (1 ml.), and evaporated to dryness. The colour should be white or faintly pink. A reddish-brown colour would indicate the presence of iron, and the need of a repetition of the above procedure. To mount a sample, the oxalate was redissolved in about 0.2 ml. of concentrated HCl, and placed in the crucible hole a drop at a time, evaporating each to dryness before the next.

2. Operating Conditions

The crucibles used are made of 1/16 inch diameter tantalum wire, 1/4 inch long. In one end a hole is drilled to receive the sample. For the 2 mg. samples of neodymium filings this was 0.035" in diameter, 1/8 inch deep; for the oxalate, it was about 0.05 inches in diameter and only 1/32 inch deep. The crucibles are either squeezed on, or welded, to a 0.02 inch tungsten wire, about one inch in length, which is clamped into the permanent support with a set screw. The position of the crucible with respect to the shield and the tungsten filament, and its relative size, are shown in Figure 1. The crucibles were set as close as electrical insulation would permit to the hole in the cap of the shield lining ($0.002" < \text{clearance} < 0.010"$). The filament which supplied the bombarding current was in a plane approximately 0.01" behind the open end of the crucible.

The operating range for the current of bombarding electrons, which are accelerated to 500 volts, depended on the sample. The larger samples of metal filings required from 10 to 25 ma., while the oxalate samples gave satisfactory peaks between 15 and 40 ma. The most usual currents were 13 ma. and 30 ma. respectively.

To record the ion currents reaching the Faraday collector, a D.C. amplifier and Brown recorder are used, as described by Horsley[14]. The output of the amplifier is relayed to the recorder through a series of shunts which permits signal reductions of approximately one third, one ninth, etc. Under the conditions specified above peaks for Nd^{142} (27%) were obtained on the second, and sometimes the third shunt, corresponding to an approximate decrease in sensitivity of 3 and 9 respectively.

With the source filament off, the apparatus could be pumped down to a pressure of about 7×10^{-6} mm. of Hg. However, with the source in operation, the pressure increased. At the lowest obtainable bombarding electron current, the best vacuum was about 1×10^{-5}. As the electron current was raised, the pressure also rose until, at 20 or 30 ma., it became 2 to 3×10^{-5} mm. of Hg. For future precision work, resolution could be improved considerably by the addition of an extra diffusion pump at the source end.

3. Peak Shape, Resolution

As shown in Appendix B, the resolution and peak shape depend on the sum and ratio, respectively, of the slit widths at source and collector. The peak height will be a maximum for a given resolution, when the collector slit is the same width as the image of the source slit after deflection. However, since such a peak is triangular in shape, coming to a point at the top, determinations of relative peak heights are too dependent on the zero signal fluctuations of the D.C. amplifier, and the recorder "lag", to yield the degree of accuracy required in this work. Satisfactory results were obtained when the width of image of the slit was 60%, or less, of the width of the collector slit, or vice versa.

For the slit widths used in these experiments (S_{source} = 0.010 cm., $S_{collector}$ = 0.016 cm.) the theoretical resolution is 1 part in 340. By extrapolating the straight sides of the peaks (Figure 4) to the zero line, the resolution was measured as 1 part in 370. This high degree of resolution was found to be necessary because of broadening at the base of the peak due to ion scattering in the electrostatic and magnetic analysers

at excessive pressure. The degree of overlapping of the broadened bases of adjacent peaks will depend on the extent of the individual "tails". Any overlapping of the "tails" will mean that the minima between adjacent peaks will not reach the zero line. If however, the "tail" of a large peak has a measurable height at the centre of the next peak, the latter will appear larger than it actually is.

The first case, of moderate overlapping, is only serious for the most sensitive shunt, since only there is the drift of the zero line measurable. This difficulty was overcome by joining the base line on both sides of the peaks being measured (see Figure 4) and determining a correction factor proportional to the deviation of the minima from this straight line.

Correction in the second case cannot yield results of sufficient accuracy for this work. It was therefore necessary to ensure that the resolution was sufficient to separate two adjacent peaks by an amount at least equal to the extension of the "tail". Measurements on the extent of the broadening for isolated peaks, under the conditions which applied in these experiments, indicated that the resolution must be 2½ times that required for unbroadened peaks. For neodymium this would be 1 part in 370, in excellent agreement with the measured value.

V RESULTS

1. Treatment of Results

(a) Measurement of Peak Hts: Because of the overlapping of "tails", (see figure 4) with resultant masking of the zero line, the following correction was added to each peak: The zero line below mass 140 (A & A′ on Figure 4) was joined to the line at mass 147 (B & B′ on Figure 4) where there is no peak. The deviations from this line of the minima between peaks were added algebraically (a,b---e, a′,b′---e′) (positive if the zero line is not crossed, negative if it is). Except for a very few runs this sum was definitely positive. The mean deviation per set was then determined, and this was distributed in proportion to the sum of the adjacent peaks (i.e. the value assigned to (b+b′) would be greater than that assigned to any other pair of minima). The correction factor added to each peak, then, would be the mean of the value assigned to the adjacent minima.

The peak heights proper are measured from the line joining adjacent minima. The line JK (Figure 4) for example, is the uncorrected height of the one Nd^{142} peak.

(b) Calculation of Relative Abundances: The peaks corresponding to the seven isotopes are scanned by varying the magnet current. A "set" consists of an "up-scan" and a "down-scan", corresponding to an increasing, and a decreasing, magnet current, respectively. A "run" is a succession of 10 or 12 sets. To determine the relative abundances, the summed peak height corresponding to each mass is determined, multiplied by the shunt factor when less sensitive shunts are used. A summed peak height is the

FIG. 4 - SAMPLE SET OF NEODYMIUM PEAKS (OXIDE)

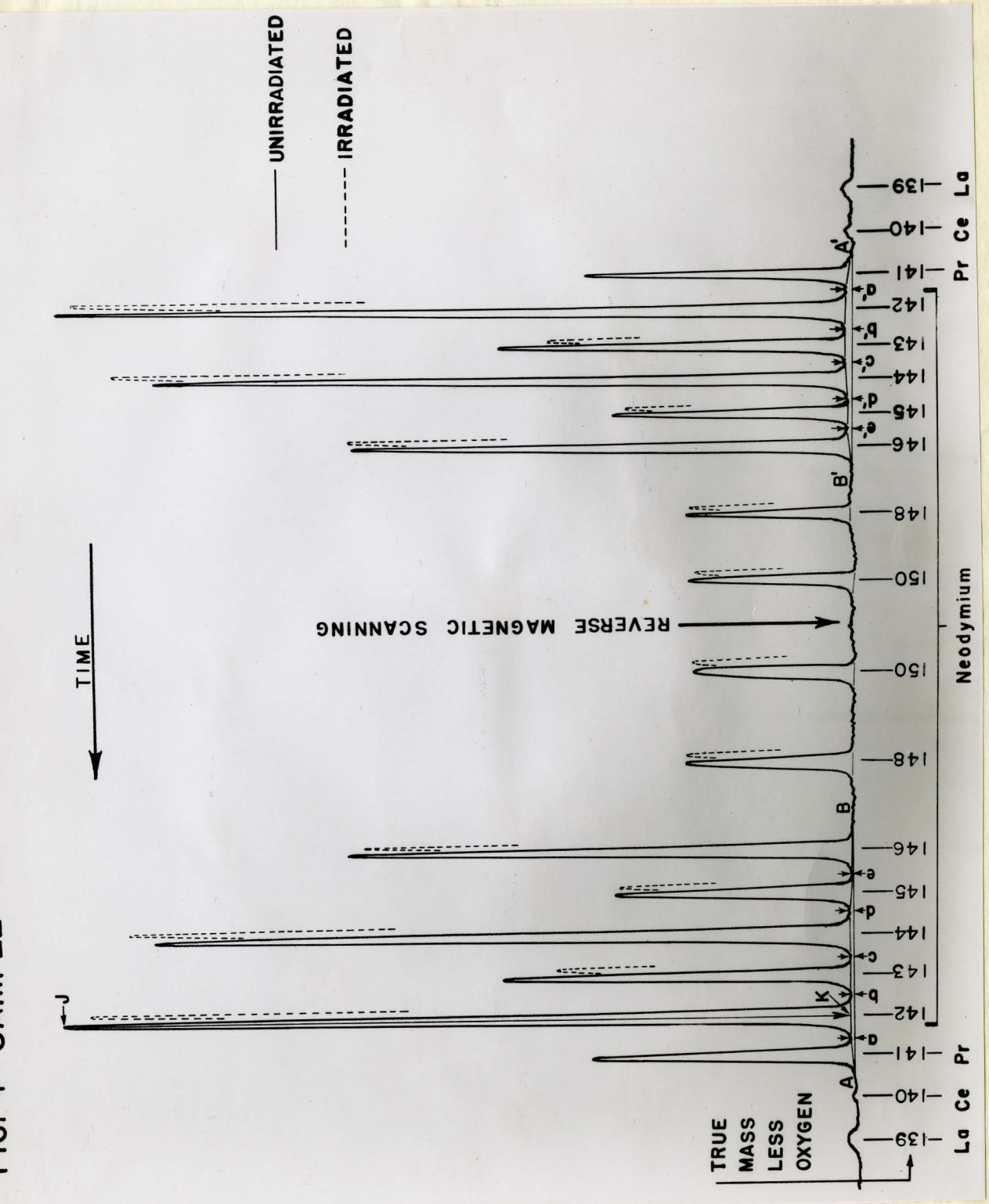

total of the measured peak heights for both the "up and down-scan" for a particular isotope, plus the proper correction factor. The relative abundance of a given isotope in a "set" is then the ratio of the appropriate summed peak height to the total of all seven summed peak heights in that "set".

The mean values for any run are the arithmetic means of all the "set" abundances corresponding to each isotope, using the rejection criterion that the deviation of any value from the mean (not including the "set" abundance in doubt) must be less than twice the standard deviation. These are the values reported in the tables which follow.

The final result for each type of sample (irradiated or not, filings or oxalate) are obtained by taking the mean of the tabulated results, which number six or more.

2. UNIRRADIATED NEODYMIUM - METAL FILINGS - TABLE I

With a single exception (sample (g) in Table I) these samples yielded two runs or less. The change in isotopic abundances between runs on the same sample was much larger than the standard deviations, and in a direction corresponding to some form of mass fractionation*. It seemed advisable, therefore, to average all results for each sample in determining the standard deviation of the mean. When this was done the results were in excellent agreement. In taking the mean of all these values, it was found that only one had to be rejected - that for Nd^{150} in sample (d).

---

*The lightest isotope, Nd^{142}, decreased with use, while the three heaviest, $Nd^{146, 148, 150}$ increased relatively. Note that the atomic weight, or "centre of mass" for neodymium is 144.3.

The standard deviations (in brackets) for these final values check well with the statistical formula that the standard deviation of a mean is equal to the standard deviation of each observation, divided by the square root of the number of observations (sets in a run).

TABLE I - RESULTS FOR UNIRRADIATED NEODYMIUM (FILINGS)

Sample	Run No.	Percent Relative Abundances Nd^{142}	Nd^{143}	Nd^{144}	Nd^{145}	Nd^{146}	Nd^{148}	Nd^{150}
(a)	1	27.10(9)	12.15(5)	23.85(6)	8.27(3)	17.24(6)	5.76(5)	5.61(7)
(b)	1	27.12(9)	12.12(6)	23.82(7)	8.29(5)	17.25(8)	5.74(6)	5.66(4)
(c)	1	27.27(11)	12.18(5)	23.92(8)	8.25(5)	17.18(7)	5.65(6)	5.55(6)
	2	26.93(11)	12.08(6)	23.83(6)	8.32(6)	17.35(6)	5.78(5)	5.71(5)
(d)	1	27.16(9)	12.14(4)	23.86(6)	8.26(3)	17.19(6)	5.73(4)	+5.65(5)
	2	26.95(11)	12.14(7)	23.83(8)	8.29(5)	17.29(9)	5.80(5)	+5.70(5)
(e)	1	27.05(9)	12.17(4)	23.81(6)	8.30(4)	17.25(7)	5.73(4)	5.60(3)
(f)	1	27.27(8)	12.20(4)	23.79(9)	8.29(5)	17.21(6)	5.71(6)	5.58(3)
	2	26.94(7)	12.08(6)	23.86(4)	8.26(6)	17.34(6)	5.81(5)	5.71(6)
(g)	1	27.14(7)	12.17(5)	23.82(7)	8.26(5)	17.24(4)	5.72(2)	5.62(5)
	2	27.08(5)	12.15(4)	23.85(5)	8.29(5)	17.28(7)	5.74(3)	5.63(4)
	3	27.08(11)	12.12(7)	23.75(4)	8.31(4)	17.29(8)	5.79(3)	5.70(5)
MEAN		27.09	12.14	23.83	8.28	17.26	5.74	5.63
*Std.Dev.		.025	.017	.024	.011	.017	.016	.023

* The std. dev. is determined by the deviations of the averages for each individual sample from the mean value.

+ These values are rejected because their average differs from the mean value by more than 2 x std. dev.

3. UNIRRADIATED NEODYMIUM - OXALATE - TABLE II

The effect attributable to mass fractionation was only slight with these much smaller samples, even after six runs. Rather than attempt to fit the results with a consistent set of lines (fitted by least squares) which would take this into account, it was decided to take the means instead. The standard deviations, at least for the extreme masses, cannot be expected to compare with the previous results.

TABLE II - RESULTS FOR UNIRRADIATED NEODYMIUM - OXALATE

Run No.	Percent Relative Abundance						
	Nd^{142}	Nd^{143}	Nd^{144}	Nd^{145}	Nd^{146}	Nd^{147}	Nd^{148}
1	27.12(17)	12.16(5)	23.84(9)	8.33(2)	17.20(5)	5.71(4)	5.63(5)
2	27.09(6)	12.12(3)	23.85(3)	8.32(4)	17.25(4)	5.76(2)	5.66(2)
3	27.00(6)	12.16(4)	23.82(5)	8.31(4)	17.26(4)	5.80(3)	5.68(3)
(4)	27.10(6)	12.18(4)	23.81(5)	8.32(6)	17.20(5)	5.76(3)	5.65(3)
5	27.07(7)	12.13(5)	23.84(6)	8.30(5)	17.31(7)	5.74(2)	5.63(3)
6	26.97(5)	12.15(6)	23.89(4)	8.33(4)	17.29(6)	5.76(5)	5.66(5)
MEAN	27.06 ± .050	12.15 ± .023	23.84 ± .027	8.32 ± .012	17.25 ± .045	5.76 ± .030	5.65 ± .020
rrect'd for O^{18}	27.10 ± .050	12.16 ± .023	23.82 ± .027	8.31 ± .012	17.22 ± .045	5.74 ± .030	5.65 ± .020

The dominant peaks from neodymium oxalate appear around mass 160, corresponding to the singly-charged monoxide. With the metallic samples, the peaks measured were due to singly charged neodymium. Before comparing

the two results, it is necessary to correct for the presence of O^{18}, which will enhance the peaks at mass 160($Nd^{142}O^{18}$) and up. The results corrected for 0.02% of O^{18} are included in Table II. It can be seen that they agree very well indeed with the former set of results (Table I).

4. IRRADIATED NEODYMIUM - OXALATE - TABLE III

Two samples of the irradiated neodymium each yielded 6 runs. In both cases the change attributable to mass fractionation became too large, particularly for Nd^{142} and Nd^{146}, to permit satisfactory treatment by the method previously used. In view of the fact that the sample of unirradiated neodymium (oxalate) showed no serious change, even after 6 runs, and since, in addition, these results were in excellent agreement with those obtained with the filings, it was decided that the last two results from each sample of irradiated neodymium should be rejected, on the grounds that they arose from a marked diminution of the samples, and that their inclusion would lessen, rather than increase, the validity of the comparison leading to the determination of isotopic cross-sections.

As with the preceding oxalate sample the results required correction for 0.02% O^{18}. The corrected results are also included in Table III.

TABLE III - RESULTS FOR IRRADIATED NEODYMIUM - OXALATE

Sample	Run No.	Percent Relative Abundance Nd^{142}	Nd^{143}	Nd^{144}	Nd^{145}	Nd^{146}	Nd^{148}	Nd^{150}
(a)	1	26.86(8)	10.52(6)	25.64(7)	8.19(9)	17.40(9)	5.75(4)	5.63(6)
	+2	26.87(8)	✱10.49(3)	✱25.48(9)	8.15(4)	✱17.54(8)	5.76(5)	5.66(2)
	3	26.92(15)	10.55(7)	25.66(4)	8.18(7)	17.39(9)	5.72(3)	5.61(6)
	4	26.87(10)	10.52(9)	25.64(9)	8.16(8)	17.43(7)	5.76(4)	5.68(3)
(b)	+1	26.94(8)	10.59(4)	25.61(5)	8.15(2)	✱17.32(4)	5.72(3)	5.62(3)
	2	26.96(7)	10.57(2)	25.59(5)	8.16(4)	17.39(7)	5.75(3)	5.62(3)
	3	26.86(11)	10.57(5)	25.57(7)	8.18(6)	17.36(6)	5.76(4)	5.68(3)
	4	26.85(11)	10.56(6)	25.61(5)	8.14(3)	17.43(8)	5.75(4)	5.65(3)
MEAN		26.89 ± .042	10.56 ± .028	25.62 ± .033	8.16 ± .015	17.40 ± .027	5.75 + .010	5.64 ± .028
Corr'c't'd for O^{18}		26.93 ± .042	10.57 ± .028	25.61 ± .033	8.15 ± .015	17.37 ± .027	5.73 ± .010	5.64 ± .028

✱ Rejected Results

\+ Where one or more values are rejected, the remainder are adjusted so that $\sum$remainder = 100% less accepted mean of rejection.

5. Isotopic Capture Cross-Sections For Pile Neutrons

(a) First Order Approximation - As discussed in section B, the simplified expressions are valid if $\Delta n / n \ll 1$. As a first approximation, therefore, all cross-sections have been calculated using equation (5). Values of Δn, $\sum_{s=142}^{\int} \Delta n_s$, and σNt are tabulated in rows 3,4, and 5 of Table IV.

TABLE IV - ISOTOPIC CAPTURE CROSS-SECTIONS

Row No.	Quantity	Neodymium Isotopes 142	143	144	145	146	148	150
1	n	27.09 (.025)	12.14 (.017)	23.83 (.024)	*8.29 (.011)	17.26 (.017)	5.74 (.016)	5.63 (.023)
2	n′	26.93 (.042)	10.57 (.028)	25.61 (.033)	8.15 (.015)	17.37 (.027)	5.73 (.017)	5.64 (.028)
3	Δn	0.16 (.05)	1.57 (.033)	-1.78 (.04)	0.14 (.019)	-0.11 (.032)	0.01 (.023)	-0.01 (.036)
4	$\sum_s \Delta n_s$	0.16 (.05)	1.73 (.06)	-0.05 (.07)	0.14 (.02)	+0.03 (.036)	0.01 (.023)	-0.01 (.036)
5	σ Nt x100	0.59 (.18)	15.2 (.5)	-0.20 (.29)	1.7 (.24)	0.17 (.21)	.17 (0.4)	-0.17 (.63)
6	σ	14 (5)	361 (13)	<7	40 (6)	<9	<14	<11
7	Contrib to σ_c	3.8	43.9	*′	3.3	*′	*′	*′
8	Revised σ (exact)		365±13					

* Mean value from Tables I & II. All others are from Table I.

*′ All others contribute a total of 1.0 barns.

Since the total capture cross-section of Nd is known [19]* it is possible to determine the absolute capture cross-sections, as well as the integrated flux, Nt. Row 6 shows the capture cross-sections so determined, while row 7 shows the contribution of each isotope to the total.

* Using a boron standard (710 barns at a neutron energy of 0.025 ev.) the cross-section was found to be 52 barns. See also the "Discussion" (sect. VI).

The errors bracketed after each value are standard deviations. The standard deviation of a sum or difference is taken equal to the square root of the sum of the squares of the standard deviations of each part of the sum.

(b) Exact Calculation - If $\Delta n / n \ll 1$, it is necessary to use the exact formulae of appendix A. For the most obvious case, viz. Nd^{143}, which changes by 13%, the equation for the cross-section is

$$\sigma_{143}{}^{Nt} = \ln\left[n_{143} + \frac{n_{142}\,\sigma_{142}}{\sigma_{142} - \sigma_{143}}\right] - \ln\left[n'_{143} + \frac{n'_{142}\,\sigma_{142}}{\sigma_{142} - \sigma_{143}}\right]$$

The logarithm will not be sensitive to small changes in σ_{142} and σ_{143}, so that the values from row 6 of Table IV can be used. The equation then gives

$$_{143}{}^{Nt} = 0.1534$$

The change is about one third the std. deviation of the value resulting from the previous calculation, and corresponds to an increase in isotopic cross-section from 361 to 365 barns. There is no effect on the other values. For the remainder, which underwent much smaller changes, the first order calculation was sufficient.

6. Corrections for Gains and Losses of Neodymium

As mentioned in Section II above, the validity of the substitution of percent abundances in place of numbers of atoms is conditional on whether the total number of Nd atoms remains the same.

Gains:

The only contamination detected which could yield a neodymium isotope due to irradiation is praseodymium (Pr^{141}). This element has

a capture cross-section of 11.2 barns[19], by the pile oscillator method. The product of capture, Pr^{142}, with a 19 hr. half-life, will have decayed completely to Nd^{142} at the time of analysis (several months after the end of irradiation).

The amount of Nd^{142} due to this process will be $n_{Pr}\sigma_{Pr}Nt$, where $n_{Pr} / n_{Nd} \times 100$ is the percent contamination due to praseodymium. A sufficient limit for the praseodymium contribution to Nd^{142} is that it should be small enough not to effect a change in the last (fourth) figure representing the abundance of Nd^{142}, i.e. less than five in the fifth figure.

$$n_{Pr}\sigma_{Pr}Nt < \frac{5}{27000} n_{142}$$

or

$$\frac{n_{Pr}}{n_{Nd}} < 5.10^{-5} / \sigma_{Pr}Nt, \text{ since } n_{142} = .27n_{Nd}$$

Using for Nt the value derivable from Table IV, 4.2×10^{20} neutrons per cm^2, gives 1% for the upper limit of the praseodymium contamination.

The amount of praseodymium present in the neodymium was determined by comparing spectra, obtained with the 21 foot grating spectrograph, of silica-diluted samples of both elements. The results indicate that the neodymium sample contains between 0.1% and 1% of praseodymium. Thus the amount of Nd^{142} contributed by neutron capture in praseodymium is neglibible.

Losses:

Whenever the product isotope in the capture process is unstable there will be some loss of atoms to the element. The amount lost will

depend both on the amount formed, hence on the cross-section of the target isotope and the integrated flux, and on the amount which has decayed to another element, involving the ratio of the half-life of the product to the time between irradiation and measurement.

The three radioactive products of radiative neutron capture in neodymium are Nd^{147}, Nd^{149}, Nd^{151}. All have short half-lives, the longest being 11 days (Nd^{147}). Losses due to capture in Nd^{146}, Nd^{148} and Nd^{150} will be complete, because the interval from irradiation to measurement was much longer. The values for $\sum_s \Delta n_s$ (row 4, Table IV) for these three isotopes indicate that only for Nd^{146} is the possibility of loss appreciable. Here it is possible that the yield of Nd^{147} was as great as 0.07%. This upper limit corresponds to a cross-section for Nd^{146} of about 10 barns, and will influence the values quoted in row 6 of Table IV by only one half the standard dev. However, even this possibility seems improbable in view of the value of 1.86 obtained by Bothe[11] (see Table V).

7. OTHER CONTAMINATIONS

In addition to the praseodymium peak, which appears at mass 141, and, as the oxide, at mass 151, with heights varying from (1/10)th to (1/3)rd that of Nd^{142}, small peaks appeared at masses 139, 140, 155, 156, 165 and 181.

Masses 139 and 155

Maximum height of both was 0.3 cm. Only two elements are possible at mass 139, lanthanum and tellurium (oxide). The latter is ruled out because of the small relative abundance of Te^{123} (0.9%) for

if this were detectable, the TeO contribution at masses 142, 144 and 146 would be very large (up to 12 cm, or about 100% at Nd^{146}) seriously altering the neodymium distribution.

At mass 155, peaks may be due to $La^{139}O$, or Gd^{155} (15%). The gadolinium can be ruled out for two reasons. First, it could only affect the neodymium oxide ratios. Since these are in good agreement with the neodymium metal results, the presence of gadolinium, if any, would require a peak at mass 155 much smaller than that observed. Secondly, in the neodymium dioxide region (about mass 175) there were no traces of gadolinium oxide, even though the neodymium peaks were only a few cm. high. Preliminary work on GdO, done prior to the work with neodymium, indicated that the oxide peaks were more than twice the size of the singly-ionized gadolinium peaks. This result agrees with the general results for all elements yet noted in this region. Failure to detect GdO peaks, therefore, rules out Gd^{155} as a contributor.

Thus lanthanum and lanthanum oxide can be the only contaminants giving these peaks. Their presence cannot affect the results.

Masses 140 and 156 (maximum height 0.15 cm.)

The ions of Ce^{140}(88%), $Te^{124}O$ (4.6%) or $Sn^{124}O^{16}$ (6%) can contribute to the mass 140 peak. The latter can be ruled out by the absence of measurable peaks at lower masses. For example, at mass 136, the $Sn^{120}O^{16}$ peak would be about 1 cm. high. Tellurium has been ruled out previously.

At mass 156, contaminants may be $Ce^{140}O^{16}$, Gd^{156}(21%) or Dy^{156}(0.05%). The dysprosium is readily ruled out, since a detectable peak at mass 156 would require one about 60 cm. in height mt mass 163, between $Nd^{146}O^{16}$

and $Nd^{148}O^{16}$. The gadolinium has been discounted previously.

Both peaks can be attributed to the presence of cerium and its monoxide. Fortunately, the amount of Ce^{142}, which overlaps Nd^{142}, will be undetectable, since Ce^{142}: Ce^{140}:: 1:8, giving a maximum peak height of 0.02 cm. at mass 142. Even if this did influence the Nd^{143} results (unlikely, since it is much smaller than either the correction factor, or the standard deviation for an individual "set" result), the change due to irradiation would be much too small to detect.

Masses 165 and 181 (maximum heights: 0.1 cm. at 165, 5 cm. at 181)

These two peaks, at 165 and 181, can only be due to holmium (165), which has a capture cross-section of 65 barns. After irradiation and decay, the product, Er^{166}, will be about 0.03 as abundant as holmium. If erbium has an ionization efficiency of the order of 30 times that of holmium this contribution would appreciably affect the abundance of irradiated Nd^{150} (oxide). Such a possibility is ruled out by a survey of the mass range 140 to 200 at 46.5 ma. At this current the holmium peak had increased in size to 1/3 that of Nd^{150}, while that of its oxide is more than ten times as large, and of the dioxide even larger. There was no sign of erbium peaks next to any one of these three peaks. Thus the presence of this contaminant also leaves the percent abundances unaffected.

VI DISCUSSION

The values for the isotopic abundances obtained with the unirradiated neodymium agree well with previously published results,[20,21] These are compared in Table V.

Isotopic Mass No.	Percent Abundances		
	Present Work	Ingraham, Hess & Hayden[20]	Mattauch & Scheid[21]
142	27.09 ± .03	27.13	26.80
143	12.14 ± .02	12.20	12.12
144	23.83 ± .03	23.87	23.91
145	8.29 ± .01	8.30	8.35
146	17.26 ± .02	17.18	17.35
148	5.74 ± .02	5.72	5.78
150	5.63 ± .02	5.60	5.69

TABLE V ISOTOPIC ABUNDANCES FOR NATURALLY-OCCURRING NEODYMIUM

The differences between these three sets of results show the effect previously attributed to isotope fractionation. In particular, the more divergent results of Mattauch and Scheid show much better agreement with the values obtained in the second runs with samples (c), (d), and (f) (unirradiated neodymium - Table I) than with the other two columns of Table V.

In Table VI the final results of this experiment are compared with those previously reported. The values for Nd^{146} and Nd^{148} which

were obtained by activation methods[11] are referred to holmium. Those obtained mass-spectrometrically are relative. Hess and Ingrham[10] based their isotopic cross-sections on a value of 45 barns for σ_c in neodymium. For purposes of comparison, the present results are given for a total capture-cross section of both 52 and 45 barns.

Comparison of results from different sources cannot be expected to agree very closely when it is recalled that non-resonance capture varies inversely as the neutron velocity, or as the square root of the neutron energy , and that the energy distribution will differ between piles. If considerable resonance capture occurs in the epi-cadmium energy range, where neutron distribution differences will be more pronounced, comparison becomes meaningless unless corrections are made. Fortunately neodymium shows no resonance capture between 0.04 ev. and 10 ev.[22].

The absence of resonance capture makes the discrepancy between the two most recent published values of 44 barns[23] and 52 barns[18] difficult to reconcile, since both were obtained using the pile oscillator technique. At Oak Ridge[23], the measurements were made in the pile shield, where the distribution of neutron energies is entirely in the thermal range. The Argonne[18] results were obtained inside the pile itself, and will therefore contain the contribution due to resonance capture. In addition, the Oak Ridge group[23] based their results on a standard of 95 barns for gold while the latter used 710 barns for boron (both at 0.025 ev). While it is true that the Argonne results tend to be higher than those from Oak Ridge, this is not always the case. In particular, the latter

obtain 730 barns for boron. This value lies within the quoted 5% deviation of the standard value used by Harris, et al. The discrepancy for neodymium, which is believed to follow the 1/v law, as boron does, is difficult to explain.

TABLE VI - COMPARISON OF RESULTS

Isotopic Mass No.	Present Results σ_c = 52b	σ_c = 45b	Hess & Ingraham[10] σ_c = 45b	* Bothe[11] σ_c = 64b(Ho)
142	14 ± 5	12 ± 4	< 12	
143	365 ± 13	316 ± 11	240	
144	< 7	< 6	< 15	
145	40 ± 6	35 ± 5	<30	
146	<9	< 8	< 20	1.8
148	<14	<12	< 45	3.7
150	<11	<10	< 45	

* Bothe's original work was based on a value of 49b for σ_c of Ho^{165}. The activation cross-sections listed here have been corrected for σ_c = 64b for Ho^{165}, as quoted by Pomerance[23].

APPENDIX A

THEORY OF ISOTOPIC CROSS-SECTIONS FOR PILE NEUTRONS

An element of charge Z has isotopes with mass numbers A + 1, A + 2, ----- A + n, of which at least the first is stable and occurs naturally. These isotopes are present in the amounts n_1, n_2, -----, n_n nuclei per c.c. before irradiation, and n_1', n_2', ----, n_n' nuclei per c.c. after irradiation, having undergone a change of Δn_1, Δn_2, ---, Δn_n nuclei per c.c., where $\Delta n = n - n'$. This change is due to the capture of neutrons in a flux of N per cm^2 per sec. for a time t seconds, where the capture cross-sections are σ_1, σ_2, ---, σ_n respectively.

The basic equations are those for the number of atoms present in a radioactive decay chain after a time t. These are

$$n_1' = n_1 e^{-\lambda_1 t}$$

$$n_2' = n_1 \lambda_1 \left[\frac{e^{-\lambda_1 t}}{\lambda_2 - \lambda_1} + \frac{e^{-\lambda_2 t}}{\lambda_1 - \lambda_2} \right]$$

(A1)

$$n_3' = n_1 \lambda_1 \lambda_2 \left[\frac{e^{-\lambda_1 t}}{(\lambda_2 - \lambda_1)(\lambda_3 - \lambda_1)} + \frac{e^{-\lambda_2 t}}{(\lambda_1 - \lambda_2)(\lambda_3 - \lambda_2)} + \frac{e^{-\lambda_3 t}}{(\lambda_1 - \lambda_3)(\lambda_2 - \lambda_3)} \right]$$

$$\vdots$$

$$n_s' = n_1 \lambda_1 \lambda_2 \cdots \lambda_{s-1} \left[\frac{e^{-\lambda_1 t}}{(\lambda_2 - \lambda_1)(\lambda_3 - \lambda_1)\cdots(\lambda_s - \lambda_1)} \cdots + \frac{e^{-\lambda_s t}}{(\lambda_1 - \lambda_s)(\lambda_2 - \lambda_s)\cdots(\lambda_{s-1} - \lambda_s)} \right]$$

The only change required in dealing with neutron cross-sections is to replace λ by σN, a permissible step since both represent the probability of the loss of a nucleus per second.

For the first (lightest) isotope, the equation is very simple,

since nuclei are lost, but none are gained from preceding isotopes.

(A2) $$n_1' = n_1 e^{-\sigma_1 N t}$$

For the remaining isotopes, it is necessary to treat each preceding isotope as the parent of a "capture" chain, in addition to the nuclear loss equivalent to equation (A2)

(A3) $$n_2' = n_2 e^{-\sigma_2 N t} + n_1 \sigma_1 \left[\frac{e^{-\sigma_1 N t}}{\sigma_2 - \sigma_1} + \frac{e^{-\sigma_2 N t}}{\sigma_1 - \sigma_2} \right]$$

where the second part is just the second equation of (A1).

Rearranging

$$n_2' = e^{-\sigma_2 N t} \left[n_2 + \frac{n_1 \sigma_1}{\sigma_1 - \sigma_2} \right] + \frac{n_1 \sigma_1}{\sigma_2 - \sigma_1} e^{-\sigma_1 N t}$$

i.e.

(A3) $$n_2' = e^{-\sigma_2 N t} \left[n_2 + \frac{n_1 \sigma_1}{\sigma_1 - \sigma_2} \right] + \frac{n_1' \sigma_1}{\sigma_2 - \sigma_1}$$

Similarly

(A4) $$n_3' = n_3 e^{-\sigma_3 N t} + n_2 \sigma_2 \left[\frac{e^{-\sigma_2 N t}}{\sigma_3 - \sigma_2} + \frac{e^{-\sigma_3 N t}}{\sigma_2 - \sigma_3} \right] + n_1 \sigma_1 \sigma_2 \left[\frac{e^{-\sigma_1 N t}}{(\sigma_2 - \sigma_1)(\sigma_3 - \sigma_1)} + \frac{e^{-\sigma_2 N t}}{(\sigma_1 - \sigma_2)(\sigma_3 - \sigma_2)} + \frac{e^{-\sigma_3 N t}}{(\sigma_1 - \sigma_3)(\sigma_2 - \sigma_3)} \right]$$

Rearranging

$$n_3' = e^{-\sigma_3 N t} \left[n_3 + \frac{n_2 \sigma_2}{(\sigma_2 - \sigma_3)} + \frac{n_1 \sigma_1 \sigma_2}{(\sigma_1 - \sigma_3)(\sigma_2 - \sigma_3)} \right] + e^{-\sigma_2 N t} \left[\frac{n_2 \sigma_2}{\sigma_3 - \sigma_2} + \frac{n_1 \sigma_1 \sigma_2}{(\sigma_1 - \sigma_2)(\sigma_3 - \sigma_2)} \right] + e^{-\sigma_1 N t} \left[\frac{n_1 \sigma_1 \sigma_2}{(\sigma_2 - \sigma_1)(\sigma_3 - \sigma_1)} \right]$$

The second term is equal to $$\left[n_2' - \frac{n_1' \sigma_1}{\sigma_2 - \sigma_1} \right] \left[\frac{\sigma_2}{\sigma_3 - \sigma_2} \right]$$

and the third term is equal to

$$\frac{n_1' \sigma_1 \sigma_2}{(\sigma_2 - \sigma_1)(\sigma_3 - \sigma_1)}$$

Combining the two terms in n_1' gives

$$n_1'\left[\frac{-\sigma_1\sigma_2}{(\sigma_2-\sigma_1)(\sigma_3-\sigma_2)}+\frac{\sigma_1\sigma_2}{(\sigma_2-\sigma_1)(\sigma_3-\sigma_1)}\right]=n_1'\left[\frac{\sigma_1\sigma_2}{\sigma_2-\sigma_1}\left(\frac{-\sigma_3+\sigma_1+\sigma_3-\sigma_2}{(\sigma_3-\sigma_2)(\sigma_3-\sigma_1)}\right)\right]$$

$$=n_1'\frac{\sigma_1\sigma_2}{(\sigma_1-\sigma_3)(\sigma_3-\sigma_2)}$$

Therefore

(A4′)

$$n_3'=e^{-\sigma_3 Nt}\left[n_3+\frac{n_2\sigma_2}{\sigma_2-\sigma_3}+\frac{n_1\sigma_1\sigma_2}{(\sigma_1-\sigma_3)(\sigma_2-\sigma_3)}\right]+\frac{n_2'\sigma_2}{\sigma_3-\sigma_2}+\frac{n_1'\sigma_1\sigma_2}{(\sigma_1-\sigma_3)(\sigma_3-\sigma_2)}$$

Equations (A2), (A3′) and (A4′) can be rearranged to give the required expressions for the capture cross-sections.

(A5a) $$\sigma_1 Nt=\ln n_1-\ln n_1'$$

(A5b) $$\sigma_2 Nt=\ln\left[n_2+\frac{n_1\sigma_1}{\sigma_1-\sigma_2}\right]-\ln\left[n_2'+\frac{n_1'\sigma_1}{\sigma_1-\sigma_2}\right]$$

(A5c) $$\sigma_3 Nt=\ln\left[n_3+\frac{n_2\sigma_2}{\sigma_2-\sigma_3}+\frac{n_1\sigma_1\sigma_2}{(\sigma_1-\sigma_3)(\sigma_2-\sigma_3)}\right]-\ln\left[n_3'+\frac{n_2\sigma_2}{\sigma_2-\sigma_3}+\frac{n_1\sigma_1\sigma_2}{(\sigma_1-\sigma_3)(\sigma_2-\sigma_3)}\right]$$

The extension to the n th isotope, which is not required for neodymium, is

(A5n) $$\sigma_n Nt=\ln\left[n_n+\frac{n_{n-1}\sigma_{n-1}}{\sigma_{n-1}-\sigma_n}+\cdots\cdots+\frac{n_1\sigma_1\sigma_2\cdots\sigma_{n-1}}{(\sigma_1-\sigma_n)(\sigma_2-\sigma_n)\cdots(\sigma_{n-1}-\sigma_n)}\right]$$

$$-\ln\left[n_n'+\frac{n_{n-1}'\sigma_{n-1}}{\sigma_{n-1}-\sigma_n}+\cdots+\frac{n_1'\sigma_1\sigma_2\cdots\sigma_{n-1}}{(\sigma_1-\sigma_n)\cdots(\sigma_{n-1}-\sigma_n)}\right]$$

A somewhat different approach to the problem leads to a set of much simpler equations, which can be shown to be equivalent to modified first order approximations to equations (A5).

If the rate of change of abundance of an isotope is small, the abundance at any time τ after the start of irradiation ($\tau \ll t$) will differ only slightly from $n - \frac{\tau}{t}(n-n')$.

Assuming that this difference is negligible, this is equivalent to the relation,

$$\text{rate of capture} = \tfrac{1}{2}\left[\text{initial rate} + \text{final rate}\right]$$
$$= \sigma N \left(\frac{n + n'}{2}\right)$$

The total change due to capture, δn, is, then

$$\delta n = \tfrac{1}{2}(n + n')\,\sigma N t = n^{*}\sigma N t$$

Applying this formula to each isotope in turn gives

$$\Delta n_1 = \delta n_1 = n_1^{*}\sigma_1 N t$$

(A6)
$$\Delta n_2 = \delta n_2 - \delta n_1 = n_2^{*}\sigma_2 N t - \Delta n_1$$

$$\Delta n_3 = \delta n_3 - \delta n_2 = n_3^{*}\sigma_3 N t - (\Delta n_1 + \Delta n_2)$$

$$\vdots$$

$$\Delta n_n = \delta n_n - \delta n_{n-1} = n_n^{*}\sigma_n N t - \sum_{s=1}^{n-1} \Delta n_s$$

The approximate equations for the cross-sections become

$$\sigma_1 N t = \Delta n_1 / n_1^{*}$$

(A6)
$$\sigma_2 N t = \frac{\Delta n_1 + \Delta n_2}{n_2^{*}}$$

$$\vdots$$

$$\sigma_n N t = \frac{\sum_{s=1}^{n} n_s}{n^{*}}$$

In order to show that these equations correspond to a modification of the first order approximation, consider the specific case of the

second isotope (equation (A3′))

$$n_2' = e^{-\sigma_2 Nt}\left(n_2 + \frac{n_1\sigma_1}{\sigma_1-\sigma_2}\right) + \frac{n_1\sigma_1}{\sigma_2-\sigma_1}$$

where $e^{-\sigma_2 Nt} = 1 - \sigma_2 Nt + \frac{(\sigma_2 Nt)^2}{12} - \frac{(\sigma_2 Nt)^3}{13} + \cdots\cdots\cdots$

to a first approximation, then

(A7) $$n_2' = (1 - \sigma_2 Nt)\left(n_2 + \frac{n_1\sigma_1}{\sigma_1-\sigma_2}\right) + \frac{n_1\sigma_1}{\sigma_2-\sigma_1}$$

$$= n_2 - n_2\sigma_2 Nt + \Delta n_1\left(\frac{\sigma_1}{\sigma_1-\sigma_2}\right) - n_1\sigma_1 Nt\left(\frac{\sigma_2}{\sigma_1-\sigma_2}\right)$$

The last term is seen to be equal to the first order approximation for n_1 times $\left(\frac{\sigma_2}{\sigma_1-\sigma_2}\right)$.

Therefore $$\Delta n_2 = n_2 - n_2' = n_2\sigma_2 Nt + \Delta n_1\left(\frac{\sigma_2}{\sigma_1-\sigma_2} - \frac{\sigma_1}{\sigma_1-\sigma_2}\right)$$

$$= n_2\sigma_2 Nt - \Delta n_1$$

(A8) whence

$$\sigma_2 Nt = \frac{\Delta n_1 + \Delta n_2}{n_2}$$

This equation differs from its equivalent in the set (A6) in that n_2 replaces n_2^*.

Now the equation $n' = n(1-\sigma Nt)$ is seen to represent a rate of capture which is independent of time, just as was assumed in deriving equations (A6). In the first order approximation however, this rate is taken proportional to the initial abundance, which is certainly too large, and will therefore give an expression for the capture cross-section which which is too small.

Therefore, the set of equations (A6) are a modification of the first order approximation giving a more nearly correct value. As indicated in the calculation of the actual cross-sections, they are a very good approximation, even when $\Delta n / n$ exceeds ten percent.

APPENDIX B

OPTICAL PROPERTIES OF SPECTROMETER. PEAK SHAPE

A summary of the optical properties (magnification, resolution, dispersion) of a double-focussing (achromatic) system of radial electric and magnetic fields is contained in Mattauch's paper[17]. The equations relevant to the Dempster-type instrument will be used here.

Let $v = v_o (1 + \beta)$ be the velocity range of the ions

$M = M_o (1 + \gamma)$ " " mass range of the ions

b_e' be the displacement of an object point from the central line of the radial electric field, of radius, a_e , and

b_m'' be the displacement of the image of the point b_e' from the central line of the magnetic field, of radius a_m

Mattauch shows that

$$(B1) \qquad b_m'' = (K_m / a_m - 1)^{-1} \left[b_e' \left(\frac{K_e}{a_e} - 1\right) - \beta (K_e - K_m) - \gamma (K_e/2 - K_m) \right]$$

when the deflection in the two fields is in the same direction. K_m and K_e depend on the central radius, focal length, source position, and angle, of the magnetic and radial electric fields respectively. For this instrument (Figure B1)

$$K_m = 2a_m \quad \text{and} \quad K_e = a_e \left[1 - \cos \sqrt{2} \left(\frac{\pi}{2}\right) \right] + D \sqrt{2} \sin \sqrt{2} \left(\frac{\pi}{2}\right)$$

It was pointed out in section IV that velocity focussing required a specific ratio for a_m / a_e. This is equivalent to making b_m independent of velocity, (of β), i.e. $K_m = K_e$. A direct computation shows that the dimensions of the instrument fulfil this requirement (a_e = 8.48 cm., a_m = 9.72 cm., D = 5.18 cm.)

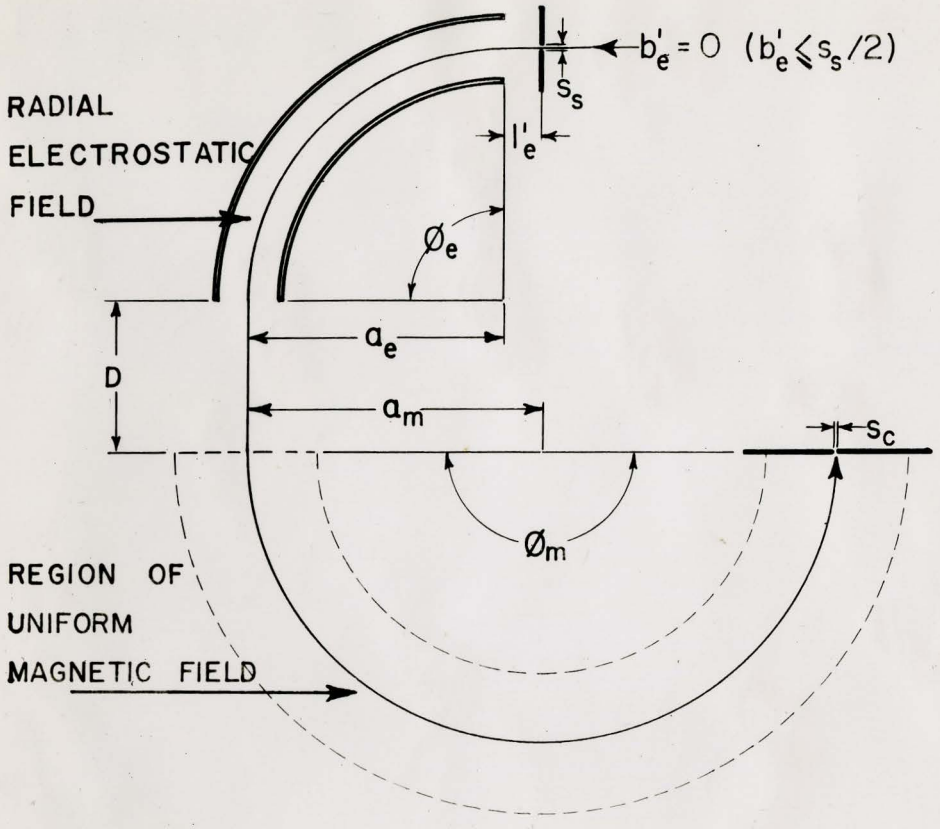

FIG. B1 - DIMENSIONS OF THE DOUBLE - FOCUSSING MASS SPECTROMETER

Magnification:

Equation (B1) will give the half-width of the image of the source slit (half width $S_s / 2$) for a single isotope ($\gamma = 0$) if we let b_e' take its max. value $S_s / 2$.

(B2)
$$b_m'' = \left(\frac{K_m}{a_m} - 1\right)^{-1} \cdot b_e' \left(\frac{K_e}{a_e} - 1\right)$$

$$= b_e' \left(\frac{2a_m}{a_e} - 1\right)$$

Thus the magnification $m = \frac{b_m''}{b_e'} = \frac{19.44}{8.48} - 1 = 1.29$

Dispersion:

The distance between the centres of two adjacent isotopic peaks (masses M_o and $M_o + 1$) is obtained from equation (B1) by setting $b_e = 0$ and $\gamma = 1/M_o$

(B3)
$$d_{(M_o)} = -\gamma\left(\frac{K_e}{2} - K_m\right) = \frac{K_m \gamma}{2} = a_m / M_o.$$

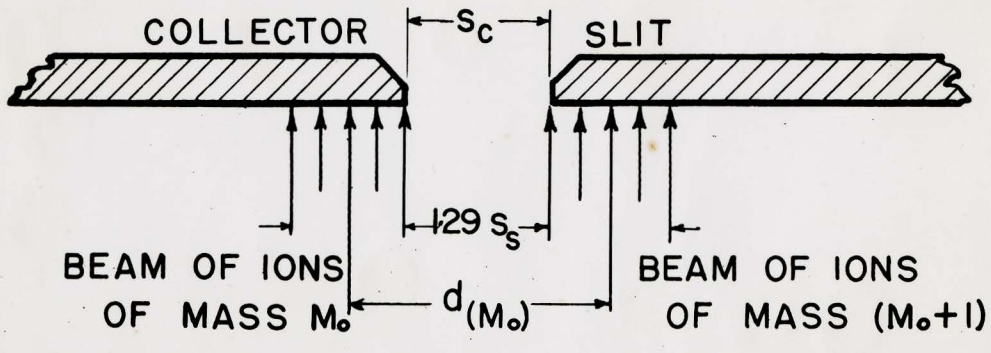

FIG. B2 – RESOLUTION OF MASS M_o IONS

Resolution:

Two peaks will just be resolved when the images of the source slit lie adjacent to, but do not overlap the collector slit (see Fig. B2). Even a small shift to either right or left will permit a part of one of the beams to register. This requires a dispersion equal to the sum of the image of the source slit, and the width of the collector slit, i.e. the resolution

(B4) $$\frac{\Delta M}{M} = \frac{1}{M_o} = \frac{1.29\, S_s + S_c}{a_m}$$

For the work with neodymium, then

$$\frac{\Delta M}{M} = \frac{0.129 + 0.16}{97.2} = 1 / 340$$

This value is in satisfactory agreement with the measured resolution of 1 / 370.

Peak Shape:

For a given width of source slit the shape of the peak recorded will depend on the width of the collector slit. Suppose the beam has the fixed width $w = 1.29\ S_s$, and has a flux of N ions per second. Three different cases will be studied: (i) $S_c = w$

(ii) $S_c > w$

(iii) $S_c < w$

(i) $S_c = w$.

Referring to figure B2, we see that the current to the collector will be zero. Let the two beams now move so that the centre line of one of them is at the edge of the slit. The collector current will be N /2. When the centre line of beam and slit coincide, the current will be N. Since the beam just "fits" the slit, the reduction in current due to a deviation, δ, of the beam will be proportional to δ. The peak will therefore be triangular in shape, pointed at the top, of height N, and will have a base equal to 2wC, where C is a constant determined by the rate of scanning (Figure B3(a)).

(ii) $S_c > w$.

In this case the collector current will be N before the centre of the beam reaches the centre of the slit, i.e., whenever the trailing edge passes the edge of the slit. It will remain this large until the leading edge of the beam passes beyond the opposite slit edge. The peak will be flat-topped, of height N, with a base of $C(w + S_c)$, which is greater than C(2w) by an amount equal to the width of the flat top.

FIG. B3 - VARIATION OF PEAK SHAPE WITH RELATIVE SLIT WIDTH

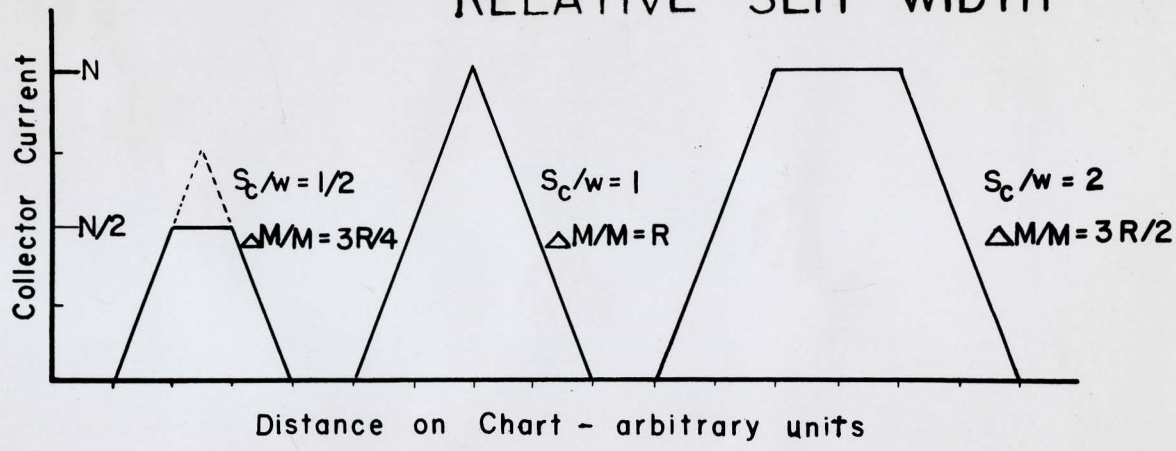

(a) CONSTANT IMAGE WIDTH

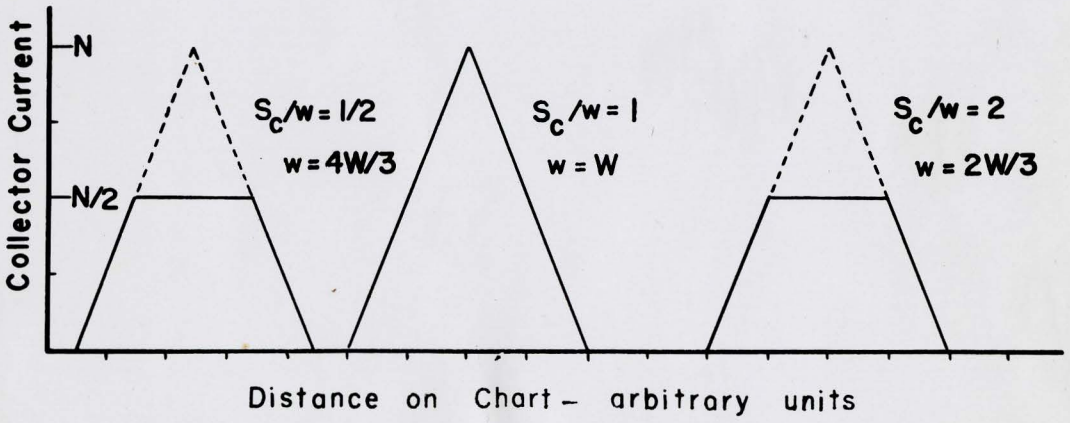

(b) CONSTANT RESOLUTION

(iii) $S_c < w$.

When the beam is centred on the slit, the current will be $N(\frac{S_c}{w})$. It will be constant at this value over a range similar to the previous case (edge of beam & edge of slit coincident). The peak will be flat-topped, of height $N(\frac{S_c}{w})$, and with base width equal to $C(w + S_c)$, in this case less than $C(2w)$. Both of these peaks are shown in Figure B3(a).

Since resolution is determined by the sum of image width and collector slit width, it is apparent that the resolution will differ for the above 3 cases. Figure B3(a) is drawn for the particular case of $S_c / w = \frac{1}{2}, 1, 2$ respectively.

Figure B3(b) shows the effect of requiring that the resolution be constant, i.e. $S_c + w = \text{const.}$

Figure B3 shows that the degree of "flatness" of a recorded peak depends on the deviation from unity of the ratio $\frac{1.29\ S_s}{S_c}$.

REFERENCES

(1) L. Seren, H. N. Friedlander and S. H. Turkel - Phys. Rev. 72, 888 (1947)

(2) J. I. Hoover, W. H. Jordan, C. D. Moak, L. Pardue, H. Pomerance, J. D. Strong, and E. O. Wollan - Phys. Rev. 74, 864 (1948)

(3) H. Pomerance & J. I. Hoover - Phys. Rev. 73A, 1265 (1948)

(4) H. Pomerance - Phys. Rev. 76A, 195 (1949)

(5) J. Rainwater and W. W. Haven - Phys. Rev. 70, 136, and 154 (1946)

(6) W. J. Sturm and G. P. Arnold - Phys. Rev. 71, 556 (1947) - L

(7) R. E. Lapp, J. R. Van Horn, and A. J. Dempster - Phys. Rev. 71, 745 (1947)

(8) A. J. Dempster - Phys. Rev. 71, 829 (1947) - L

(9) R. J. Hayden, J. H. Reynolds, M. G. Ingraham - Phys. Rev. 75, 1500 (1949)

(10) D. C. Hess, and M. G. Ingraham - Phys. Rev. 76, 300 (1949) - L

(11) W. Bothe - Z. Naturforsch 1, 179 (1946)

(12) A. J. Dempster - Proc. Am. Phil. Soc. 75, 755 (1935)

(13) A. E. Shaw - MDDC 308, A. E. C. (1946)

(14) R. J. Horsley - M. Sc. Thesis (physics) McMaster University, Hamilton, Ont. (1950)

(15) A. J. Dempster - P. R. 51, 67 (1937)

(16) R. Herzog - Zeits f. Physik 89, 447 (1934)

(17) J. Mattauch - Phys. Rev. 50, 617 (1936), 1089 (1936) - Errata

(18) S. P. Harris, C. O. Muehlhause, S. Rasmussen, H. P. Schroeder, and G. E. Thomas, Phys. Rev. 80, 342 (1950)

(19) Nuclear Data - Nat'l. Bur. Stds. Bull. 499 (Washington)

(20) M. G. Ingraham, D. C. Hess, & R. J. Hayden, Phys. Rev. 74, 98 (1948)

(21) J. Mattauch and H. Scheld - Z. Naturforsch, 3a, 105 (1948)

(22) R. K. Adair - Rev. Mod. Phys. 22, 249 (1950)

(23) H. Pomerance - Phys. Rev. 83, 641 (1951)